Seçkin D. Günay*

Investigation of Oxygen Diffusion in Irradiated UO_2 with MD Simulation

DOI 10.1515/htmp-2015-0137
Received June 12, 2015; accepted October 24, 2015

Abstract: In this study, irradiated UO_2 is analyzed by atomistic simulation method to obtain diffusion coefficient of oxygen ions. For this purpose, a couple of molecular dynamics (MD) supercells containing Frenkel, Schottky, vacancy and interstitial types for both anion and cation defects is constructed individually. Each of their contribution is used to calculate the total oxygen diffusion for both intrinsic and extrinsic ranges. The results display that irradiation-induced defects contribute the most to the overall oxygen diffusion at temperatures below 800–1,200 K. This result is quite sensible because experimental data shows that, from room temperature to about 1,500 K, irradiation-induced swelling decreases and irradiated UO_2 lattice parameter is gradually recovered because defects annihilate each other. Another point is that, concentration of defects enhances the irradiation-induced oxygen diffusion. Irradiation type also has the similar effect, namely oxygen diffusion in crystals irradiated with α-particles is more than the crystals irradiated with neutrons. Dynamic Frenkel defects dominate the oxygen diffusion data above 1,500—1,800 K. In all these temperature ranges, thermally induced Frenkel defects make no significant contribution to overall oxygen diffusion.

Keywords: oxygen diffusion, irradiation, uranium dioxide, Frenkel defect, Schottky defect, MD simulation

Introduction

In order to understand the behavior of uranium dioxide (UO_2) molecules under operating temperatures and storage conditions, it is important to examine transport properties. One of the most important transport properties is the mass transport which is diffusion. Diffusion of oxygen sublattice is an interesting property of UO_2 because oxygen ions are mobile much below the melting temperature (0.8 T_m) [1]. Moreover, oxygen ions could be mobile even at operating or storage temperatures when the crystal structure is exposed to radiation (like neutrons and α-particles). For this purpose, to understand these combined effects a series of MD simulations are designed and results are used in order to model overall oxygen diffusion in crystal and in irradiated UO_2. In this work, author is inspired by the work of Oda and Tanaka, where they studied Li diffusion of irradiated Li_2O [2]. Their diffusion model is improved by considering the effects various irradiation sources.

Molecular dynamics (MD) boxes for crystal-, vacancy-, interstitial-, Frenkel- and Schottky-defected UO_2 supercells are constructed. Their diffusion coefficients are obtained by Einstein relation from mean square displacement data. Both in stoichiometric and non-stoichiometric UO_2, thermally generated and radiation-induced defects are considered as isolated defects, which means that their transport mechanisms are operating independently from the others. As a result, diffusion of each type of defect is directly summed in order to calculate the overall oxygen diffusion.

In the literature, defect properties and self-diffusion coefficient data were investigated using MD simulation methods [3–6]. Govers [7], in a review paper, compared defect properties in detail, like formation energies of Frenkel and Schottky defects, with many types of potentials. Williams [8] used the existing interaction potentials for the MD simulation to obtain the diffusion in crystals that have grain boundaries. In addition to these many experimental diffusion, data was reported for hyperstoichiometric, hypostoichiometric and stoichiometric UO_2 [9–14]. First principle studies are also applied to UO_2 to calculate defect properties [15].

Computational methods and potential parameters

In this study, rigid-ion potential has been used in order to model the interaction of ions. Potential parameters that were developed by Yakub et al. [16] are used because they correctly predicted most of the properties of UO_2 at both solid and liquid phases. Especially static lattice properties provide a good agreement with experimental results because potential parameters were adjusted on them. Also thermal expansion of lattice and λ (superionic)

*Corresponding author: Seçkin D. Günay, Department of Physics, Faculty of Science, Yıldız Technical University, Esenler, 34210 Istanbul, Turkey, E-mail: sgunay@yildiz.edu.tr

Brought to you by | Yildiz Technical University
Authenticated
Download Date | 12/13/18 8:15 AM

transition temperature (T_c) are predicted in a good agreement with experimental data:

$$\phi_{ij}(r) = \frac{Z_i Z_j}{r} + A_{ij} e^{\left(-r/\rho_{ij}\right)} - \frac{C_{ij}}{r^6} + D_{ij}\left(e^{-2\beta_{ij}\left(r-r_{ij}^0\right)} - 2e^{-2\beta_{ij}\left(r-r_{ij}^0\right)}\right) \quad (1)$$

Equation (1) is a combination of Buckingham- and Morse-type rigid ion potentials, where they are used to model the interaction of UO_2 ions. It consists of four types of potential terms. Coulomb interaction resides in the first term of eq. (1). Second and third terms of eq. (1) are Buckingham-type potential and the fourth term is Morse-type rigid ion potential. In the first term, Z constants are effective charges of each species. Second term indicates the short-range repulsion from the Pauli exclusion principle. Repulsive strength is arranged by constants A and ρ. Third term is the attractive part called van der Walls term. Fourth term is called the Morse-type potential. r^0 is the equilibrium bond distance, D is the depth of the potential and β changes the width of the potential. Fourth term possesses both attractive and repulsive parts. All the parameters are given in Table 1.

Table 1: $Z_U = 2.2208$ and $Z_O = -1.1104$. The unit of lengths and energies are Å and eV, respectively.

	A	ρ	C	D	β	r^0
U–U	187.03	0.3422	–	–	–	–
U–O	432.18	0.3422	–	0.5055	1.864	2.378
O–O	883.12	0.3422	3.996	–	–	–

Unrealistic attraction between O–O ions may occur; so, in order to avoid such a problem an extra exponential term $F\exp(-Gr)$ is added to the potential function to harden it [17]. This term is included to add a strong repulsive interaction at short distances and does not change the bulk properties of the crystal.

MD simulations are performed with MOLDY [18]. $8\times8\times8$ supercell is constructed for the crystal structure which has 2,048 uranium and 4,096 oxygen ions. The Ewald's sum technique is used for the long-range Coulomb interactions. In this method, the long-range interaction has three parts, which are short range, long range and energy correction. By this method, long-range interactions are computed rapidly and save valuable computation times with a high accuracy. Newton equations of motion are calculated with Beeman's algorithm with the time step of 0.001 ps. The total simulation time is 100 ps, where the first 30 ps is used to anneal the system and for 70 ps data are collected in order to calculate physical properties. Beside the crystal supercell structure, Frenkel-, Schottky-, interstitial- and vacancy-defected supercells have been used to calculate properties. Perfect crystal ($U_{2048}O_{4096}$), anion vacancy ($U_{2048}O_{4095}$), cation vacancy ($U_{2047}O_{4096}$), anion interstitial ($U_{2048}O_{4097}$), cation interstitial ($U_{2049}O_{4096}$), oxygen Frenkel, uranium Frenkel ($U_{2048}O_{4096}$) and Schottky-type ($U_{2047}O_{4094}$)-defected supercell structures constructed by adding, removing or only changing the ion coordinates. Defect concentrations for anion vacancy, interstitial and Frenkel defects are 0.0244 %; for cation vacancy, interstitial and Frenkel defects are 0.0488 %; for Schottky defects are 0.0488 %. For all the MD runs, temperature is varied from 300 to 3,200 K at 50 K intervals.

Results and discussions

The model potential used in this study calculated the critical temperature as 2,600 K and the ratio of the critical temperature to the melting point ($T_m \cong 3{,}200$ K) is estimated as $T_c/T_m \cong 0.8125$ which is within the suggested range of the PbF_2-type superionic conductor [19]. The temperature dependence of oxygen diffusion coefficients D_o obtained from the slope of the time-dependent mean square displacements at each temperature is presented in Figures 1 and 2. The self-diffusion coefficient of ions is calculated by Einstein relation, where $r_{i\alpha}(t)$ is the position of the ith ion at time t,

$$\left\langle \left| r_{i\alpha}(t) - r_{i\alpha}(0) \right|^2 \right\rangle = 6Dt \quad (2)$$

Diffusion path of the ions are changed by the nearby molecules, where the path resembles a random walk. This problem was investigated by Albert Einstein and acquired an equation for Brownian motion.

Figures 1 and 2 show the diffusive behavior of oxygen ions in the perfect crystal ($U_{2048}O_{4096}$), the defective systems like oxygen vacancy, uranium vacancy, oxygen interstitial, uranium interstitial, oxygen Frenkel defect, uranium Frenkel defect and Schottky-type defect. Three separate regions can be considered from the graphs: extrinsic diffusion is assisted by irradiation-induced defects that dominate diffusion from the thermal vibrations at lower temperatures ($1{,}200 < T_e < 1{,}750$), intrinsic diffusion operates at higher temperatures ($1{,}800 < T_i < 2{,}600$), where the diffusion is formed by the thermal energy results, dynamic Frenkel defects and in the third region, superionic diffusion which occurs at temperatures between the Bredig transition and the melting (2,600 <

Brought to you by | Yildiz Technical University
Authenticated
Download Date | 12/13/18 8:15 AM

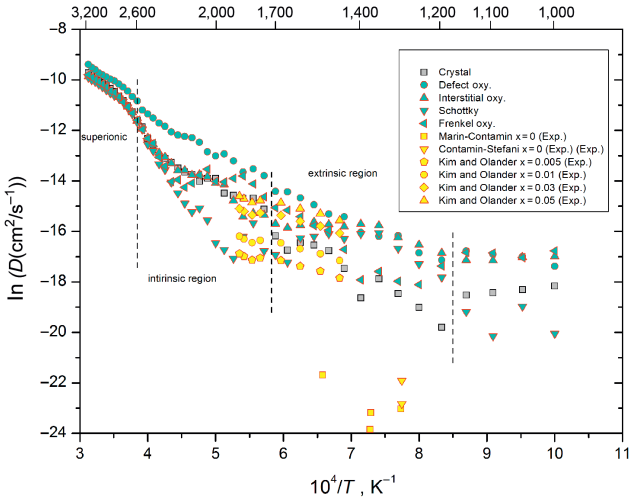


Figure 1: Oxygen diffusion calculations of oxygen vacancy, oxygen interstitial, oxygen Frenkel defect, Schottky defect and crystal supercells by MD simulations. Data are compared with experimental values.

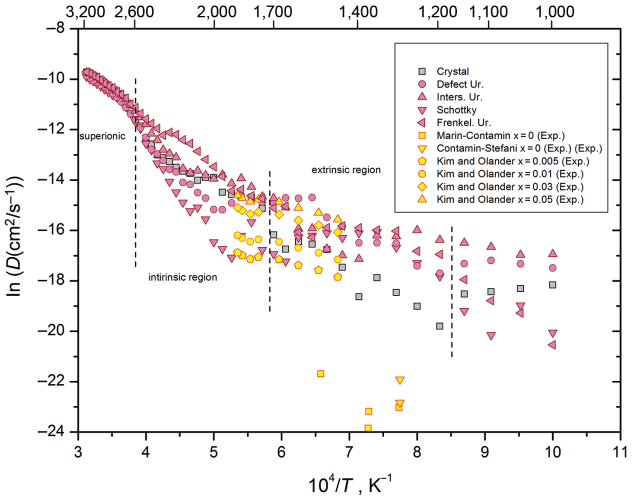


Figure 2: Oxygen diffusion calculations of uranium vacancy, uranium interstitial, uranium Frenkel defect, Schottky defect and crystal supercells by MD simulations. Data are compared with experimental values.

T_s < 3,200). In Figures 1 and 2, oxygen self-diffusion coefficients are presented at temperatures from 1,000 to 3,200 K. These graphs are plotted as ln(D) versus T^{-1} in order to display Arrhenius law:

$$D = A \times K \times (1 - K) \times \exp\left(\frac{-H}{kT}\right) \quad (3)$$

where k is the Boltzmann constant, A is the pre-exponential factor, K is the concentration of defects and the H is the activation energy of defect. For our supercell box, concentration of defects can be expressed as the ratio of number of defects to the total number of anions or cations.

In the extrinsic region, in Figure 1, oxygen diffusion is more intense in the oxygen-defected systems compared to the perfect crystal and the Frenkel-defected supercell. Also it has value comparable with the interstitial oxygen and Schottky in this region. Concentration of oxygen vacancy is 0.0244 % in the MD supercell. At low temperatures, the oxygen diffusion of Schottky type has the lowest value within the defective systems even though it has the highest defect concentration of 0.0488 %. In the case of Li_2O, this has been interpreted as occurrence of the clustering of vacancies by Oda [2], namely the clustering of O vacancies with a U vacancy in $U_{2047}O_{4094}$ reduces the oxygen diffusion. All of the defective and crystal systems, except oxygen vacancy, are approaching each other in the intrinsic region as temperature increases. The discrepancies between D_o of all defective and non-defective systems are completely dissolved in the superionic region and comparable to that of liquid state which is typical of a PbF_2-type superionics except the oxygen vacancy defect. The similar temperature dependence of the diffusion behavior of the defective and non-defective systems is also observed for Li_2O [2].

In Figure 2, almost all systems behave the same and approach to each other as the temperature is increased, like intrinsic and superionic regions. For the extrinsic part, diffusion of all types of defective systems is higher than the crystal system. Temperatures below 1,200 K are not taken into account for the extrinsic range because too much vibration of the mean square displacement data presents a huge amount of uncertainty in the slope and consequently in the diffusion data. These vibrations mainly occur because MD box is exposed to constant pressure ensemble.

The overall temperature dependence of oxygen diffusion is modeled [2] and expressed as

$$D_{\text{Oxy}} = D_{\text{radiation defects}} + D_{\text{thermally induced defects}} + D_{\text{dynamic Frenkel defects}} \quad (4)$$

Radiation defects are emerged in crystals by irradiation of fission products, α-particles, α-recoil atoms and neutrons. These extrinsic sources enhanced the diffusion of oxygen ions in the extrinsic region. Thermally induced defects were created with the increase of temperature in the extrinsic region. Dynamic Frenkel defects also appear with the increase of temperature to the critical point (~2,600 K) in the intrinsic region. This type of defect

Brought to you by | Yildiz Technical University
Authenticated
Download Date | 12/13/18 8:15 AM

eventually causes collapse of oxygen sublattice at the critical point.

Irradiation-induced defects in the extrinsic region

Radiation may affect the material and changes the crystal structure, conductivity, lattice parameter and stoichiometry as the defects are created. Radiation-induced defects are extrinsic-type defects and in this temperature range diffusion coefficient is individually evaluated from the Arrhenius plot in Figure 1 and summed in order to obtain radiation-induced diffusion as follows:

$$D_{\text{radiation defects}} = D_{\text{i_oxy}} + D_{\text{v_oxy}} + D_{\text{f_oxy}} + D_{\text{s}} \tag{5}$$

Here "i, v, f and s" denote interstitial-, vacancy-, Frenkel- and Schottky-type defects. Diffusion coefficients of each type can be summed because at low defect concentrations it is presumed that defect mechanisms operate independently. Low concentration of defects results in the absence of defect clusters.

Matzke [20] compared the properties of irradiated UO_2 samples and demonstrated that different sources have different impacts on the sample. To elucidate this idea experimental data could be observed, for example, lattice expansion of crystal due to fission [21] is almost 10 times smaller than α-irradiated [22] UO_2 sample. This huge inequality emerges from the different types of sublattice defects, fusion particles mainly create oxygen-type defects; however, α-particles create both oxygen- and uranium-type defects. This difference controls the physical properties like lattice parameter, conductivity or diffusion coefficient. For this reason, in order to evaluate diffusion induced by neutrons eq. (5) is used and for the α-particles eq. (6) is used which are given as follows:

$$D_{\text{radiation defects}} = D_{\text{i_oxy}} + D_{\text{v_oxy}} + D_{\text{f_oxy}} + D_{\text{s}} + D_{\text{i_ur}} + D_{\text{v_ur}} + D_{\text{f_ur}} \tag{6}$$

Additional components are added to eq. (5) to consider uranium defects. All these terms of the sum for eqs (5) and (6) are individually evaluated and given in Table 2.

Kim and Olander [9] obtained experimental data points of UO_{2-x} between 1,473 and 1,873 K for various oxygen vacancy concentrations such as $x = 0.005$, 0.01, 0.03, 0.05 and determined the value of activation energy 0.50736 eV and pre-exponential factor as 4.4×10^{-4} cm^2/s for concentrations $x/2$. Low x values are considered as stoichiometric UO_2. As the value of x is increased, oxygen vacancies dominate the diffusion coefficient values. In this study, both experimental and MD simulation data points divided into two parts as intrinsic and extrinsic regions: below and above 1,750 K. As a result, experimental data of Kim and Olander must be reconsidered and experimental constants are reobtained from the fit of Arrhenius plot as given in Tables 2 and 3. The activation energy of oxygen vacancy resembles the data of Kim and Olander [9]. Moreover, activation energy of crystal structure for MD is in good agreement with stoichiometric data of Marin and Contamin [10] in Table 2. Note that concentrations for crystal and Frenkel defect are taken as 1.

Table 2: A is the pre-exponential factor; H is the activation energy from the Arrhenius law.

1,200–1,700 K	A (cm^2/s)	H (eV)
$U_{2048}O_{4096}$ (crystal)	4.6×10^{-4}	1.22757
$U_{2048}O_{4096}$ (oxygen Frenkel defect)	2.5811	1.14433
$U_{2048}O_{4095}$ (oxygen vacancy)	2.2421	0.99853
$U_{2048}O_{4097}$ (oxygen interstitial)	8.1489×10^{-3}	0.34933
$U_{2048}O_{4096}$ (uranium Frenkel defect)	0.0135234	0.5016
$U_{2047}O_{4096}$ (uranium vacancy)	2.34358	1.12749
$U_{2049}O_{4096}$ (uranium interstitial)	0.0047249	0.3875
$U_{2047}O_{4094}$ (Schottky)	0.82677×10^{-3}	0.23593
Exp. ($x = 0$) (Marin and Contamin) [10]	1.711×10^{-6}	1.1525
Exp. UO_{2-x} (Kim and Olander) [9] $x = 0.005$, 0.01, 0.03, 0.05 (vacancy)	1.592×10^{-3}	0.68051

Above 1,700 K in Figure 1, both MD and experimental data demonstrate a transition region (~1,700–1,800 K) and follows an increase for the diffusion data. Figure 1 demonstrates that slope of all the data change in the intrinsic range. Murch [23] summarizes this event and concludes that as the temperature increases, a second regime appears and the slope becomes steeper in the second range. Intrinsic region is evaluated separately and following data found in Table 3.

Vacancy data is placed in Table 3 to compare with experimental value of Kim and Olander for intrinsic region. Again, activation energy for both experimental data and the MD vacancy simulation data are in good agreement. In addition to this, crystal data will be used to calculate dynamic Frenkel defects in the following sections.

Table 3: A is the pre-exponential factor; H is the activation energy from the Arrhenius law.

1,800–2,600 K	A (cm^2/s)	H (eV)
$U_{2048}O_{4096}$ (crystal)	2.906×10^{-3}	1.42556
$U_{2048}O_{4095}$ (oxygen vacancy)	17.86	1.28122
Exp. UO_{2-x} (Kim and Olander) [9] $x = 0.005$, 0.01, 0.03, 0.05 (vacancy)	2.267×10^{-2}	1.14464

Brought to you by | Yildiz Technical University
Authenticated
Download Date | 12/13/18 8:15 AM

Thermally induced defects in the extrinsic region

In the extrinsic region, both Schottky and Frenkel defects may be generated. In this region, this event occurs by thermal effects independent from a source of radiation. Thermally induced defects in the extrinsic region are neither a radiation-induced defect in the extrinsic region nor intrinsic range dynamic Frenkel defect. As a thermally induced defect, both Schottky and Frenkel defects may be taken into account but Schottky defect formation energy is higher than the Frenkel defect. For this reason, Schottky defect has limited effect and only Frenkel-type defects are taken into account. Following equation is used [2]:

$$D_{\text{thermally induced defects}} = A_{\text{i}} \times K \times \exp(-H_{\text{i}}/kT) + A_{\text{v}} \times K \times \exp(-H_{\text{v}}/kT) \quad (7)$$

$$K = \sqrt{1/2} \times \exp(-E_{\text{f}}/2kT) \quad (8)$$

Here K is the concentration of Frenkel pairs and E_{f} is the formation energy of Frenkel pairs. In order to calculate the formation energy of oxygen Frenkel pairs, Mott-Littleton [24] approach is implemented. Gulp program is used to obtain results [25]. The radii of the spheres are considered as 9 and 20 Å for Mott-Littleton approach. Radii of the region 1 and region 2a are increased until satisfactory convergence is achieved. $2 \times 2 \times 2$ supercell of UO_2 is used and oxygen vacancy and interstitial ions are placed not too close to each other to avoid direct annihilation. For this reason, a uranium ion resides between two defected sites.

Arima [3] have also calculated the formation energy of Frenkel defects for Yakub potential and found a value between 5.1 and 5.3 eV. Activation energies of oxygen from crystals with vacancy and interstitial ions at Table 2 and Frenkel defect formation energy from Table 4 (E_{f} = 5.9 eV) are used to calculate the diffusion of thermally induced defects.

Table 4: Formation energies of oxygen Frenkel pairs for various potentials from an MD study paper [7], this work and experimental data are listed.

	Arima [7]	Basak [7]	Yamada [7]	Yakub (present work)	Exp. [26, 27]
E_{f} (eV)	6.9	6.0	6.0	5.9	3.0–4.0

Dynamic Frenkel defects in the intrinsic region

As the temperature increases to the critical point oxygen ions become more mobile. At about 1,800–2,600 K, this type of Frenkel pairs is more effective than the other type mechanisms. Dynamic Frenkel pairs leave their sites gradually and contribute to total diffusion until 0.8 T_{m} [1]. Above this temperature to the melting point oxygen sublattice totally melts and behaves like a liquid where the uranium sublattice still remains like solid. Here, stoichiometric UO_2 data of MD simulation in Table 3 is taken into account to calculate diffusion coefficient.

Overall contribution to oxygen diffusion of irradiated UO_2

There are several reasons for oxygen diffusion in irradiated UO_2 fuel at different temperatures from room temperature to the melting point. These contributions consist of parts from thermal effects and radiation in the extrinsic region, in addition to this dynamic Frenkel defects in the intrinsic region. It should be noted that these contributions could be directly summed [28, 29]. It is presumed that defect mechanisms operate independently because of low-defect concentration, which means the absence of defect clusters and also nearby defects do not annihilate each other. Also these contributions have their independent effects change with the temperature. In order to observe these contributions to the total oxygen diffusion, $100 \times D_x/D_{\text{Oxy}}$ value is calculated for each part of the sum. D_{Oxy} value is given in eq. (4).

In Figure 3, at low temperatures radiation defects dominate the diffusion mechanism which means under reactor conditions, main reason for oxygen diffusion in UO_2 is fast neutrons, α-particles or recoil atoms. Radiation defect contribution (both neutron and α-particles) to diffusion dominates the overall diffusion up to ~1,200–2,000 K. Above this critical point, contribution from the dynamic Frenkel defects is observed. The effect of thermally induced defects is limited for all the temperature ranges and it has no influence on the overall diffusion and the contribution is almost zero for the irradiated UO_2. When the irradiation source changed from neutrons to α-particles the contribution of each component is changed as shown in Figure 3. It results in a considerable amount of change as indicated with the arrows. α-Irradiation-induced defects dominate the

Brought to you by | Yildiz Technical University
Authenticated
Download Date | 12/13/18 8:15 AM

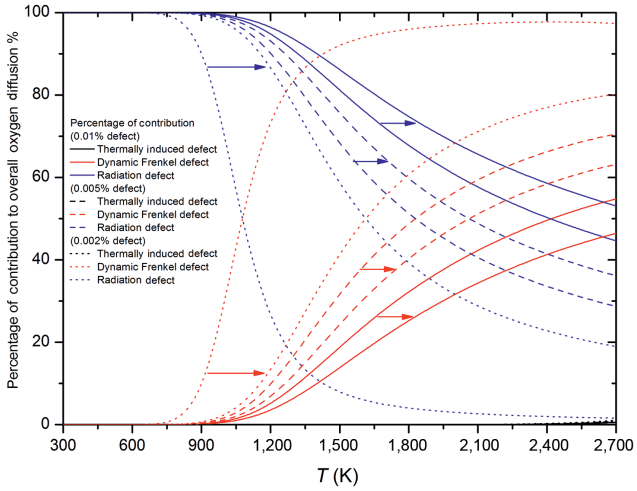


Figure 3: This figure shows the percentage of contribution to the total oxygen diffusion. If radiation source is changed from neutron to α-particles, contributions from each fragments change in the direction of the arrows.

overall oxygen diffusion for a few hundred Kelvin more than the neutron irradiation. Thermally induced defects normally should be dominant at low temperatures, but results in very small oxygen diffusion. Main reason for this in UO_2 crystal is the high value of formation energy of oxygen Frenkel pairs that results in very low concentration of these defects created with thermal effects and consequently very small diffusion coefficient of oxygen.

Radiation-induced defects consists of parts as oxygen vacancy, oxygen interstitial, oxygen Frenkel and Schottky defects. Their individual contributions to radiation-induced oxygen diffusion are observed in Figure 4.

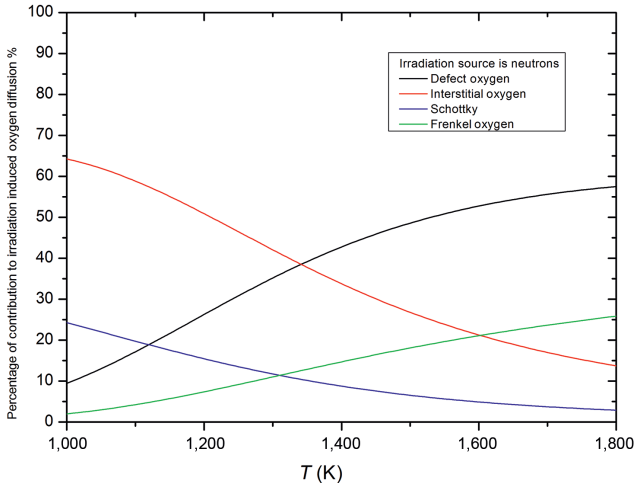


Figure 4: Contributions from oxygen vacancy, interstitial-, Frenkel- and Schottky-type defects to irradiation-induced oxygen diffusion. Here irradiation source is considered as neutrons.

Interstitial defects are more effective about 1,000 K but for higher temperatures oxygen vacancy and Frenkel defects are more operative.

In Figure 5, all types of defects contribute to the irradiation-induced oxygen diffusion. At about 1,000 K interstitial-type oxygen and about 1,800 K oxygen vacancy contribute the most to the diffusion in the extrinsic region.

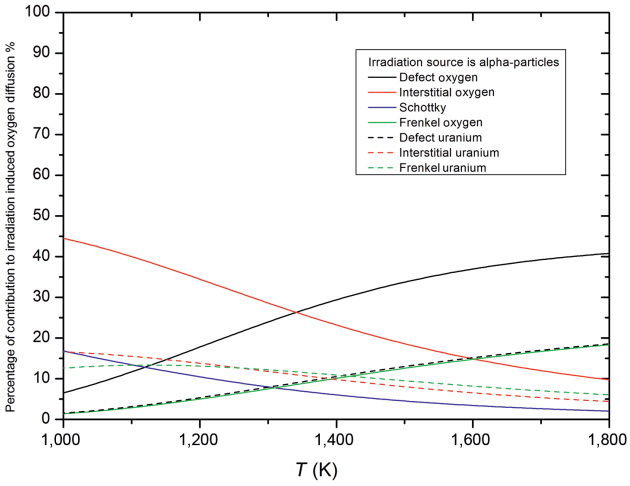


Figure 5: Contributions from oxygen and uranium vacancy, interstitial-, Frenkel- and Schottky-type defects to irradiation-induced oxygen diffusion. Here, irradiation source is considered as α-particles.

Conclusions

Physical properties like lattice parameter, electrical resistivity and diffusion of a material is changed by irradiation. Nuclear fuel or breeding blanket elements are subjected to these particles. UO_2 fuel is one of them, which is exposed to α-particles, α-recoil atoms and neutrons. As the energetic particles collide with the components of the crystal, Frenkel pairs, vacancies, interstitials and Schottky defects are created. In this paper, oxygen diffusion in UO_2 is investigated for irradiated crystal by atomistic simulation using the model of Oda and Tanaka [2]. Here, overall oxygen diffusion model is improved by considering different types of irradiation sources.

Responses of the crystal changes with the type of radiation, for example, α-particles are more effective than the others because they modify both cation and anion sublattices, whereas neutrons affect only anion sublattice of UO_2. This sublattice effect emerges from an experimental data [20], which demonstrates the effect of α-particles and neutrons on lattice parameter is very

Brought to you by | Yildiz Technical University
Authenticated
Download Date | 12/13/18 8:15 AM

different from each other. In a similar manner, overall diffusion also depends on the type of irradiation. For this reason, eq. (4) is presented to calculate overall diffusion of oxygen. In this equation, irradiation-induced diffusion part is considered as two ways: one is for neutrons (eq. (5)) and the other is for α-particles (eq. (6)). Other components of eq. (4) indicate the thermally induced defects and dynamic Frenkel defects.

MD simulations are performed from room temperature up to the melting point. All data separated into three regions as extrinsic (1,200–1,750 K), intrinsic (1,800–2,600 K) and superionic regions (2,600–3,200 K). Irradiation-induced defects dominate the diffusion in the extrinsic region and temperatures below it. In the intrinsic region, as the temperature increases from 1,800 to 2,600 K, oxygen ions are more mobile and leaving their normal sites to the new interstitial positions. Eventually dynamic Frenkel defects emerge gradually, which are more effective than the other type of defects in this temperature range. At the end of this region, oxygen sublattice totally collapses at about 2,600 K. This is an observed property of UO_2 and called as superionic transition point. From 2,600 to 3,200 K it is called the superionic region. All these parts can be observed clearly in Figures 1 and 2.

Overall contribution to oxygen diffusion at low temperatures is from irradiation-induced defects. As the concentration of these defects is increased, their range of influence increases to higher temperature points as in Figure 3. Moreover, α-particles also enhance this range. Dynamic Frenkel defects are more effective at temperatures close to the critical point. Thermally induced defects have no significant effect on the overall diffusion of irradiated UO_2 because formation energy of both uranium and oxygen Frenkel defects are very high.

Funding: This research was supported by Yıldız Technical University Scientific Research Projects Coordination Department. Project Number: 2013-01-01-GEP01.

References

[1] M.A. Bredig, Colloq. Int. CNRS, 205 (1971) 183–191.
[2] T. Oda and S. Tanaka, J. Nucl. Mater., 386–388 (2009) 1087–1090.
[3] T. Arima, K. Yoshida, K. Idemitsu, Y. Inagaki and I. Sato, IOP Conf. Ser. Mater. Sci. Eng., 9 (2010) 012003.
[4] S.I. Potashnikov, A.S. Boyarchenkov, K.A. Nekrasov and A.Y. Kupryazhkin, J. Nucl. Mater., 433 (2013) 215–226.
[5] N.-D. Morelon, D. Ghaleb, J.-M. Delaye and L.V. Brutzel, Philos. Mag., 83 (2003) 1533–1555.
[6] A.Y. Kupryazhkin, A.N. Zhiganov, D.V. Risovanyi, V.D. Risovanyi and V.N. Golovanov, Tech. Phys., 49 (2004) 254–257.
[7] K. Govers, S. Lemehov, M. Hou and M. Verwerft, J. Nucl. Mater., 366 (2007) 161–177.
[8] N.R. Williams, M. Molinari, S.C. Parker and M.T. Stor, J. Nucl. Mater., 458 (2015) 45–55.
[9] K.C. Kim and D.R. Olander, J. Nucl. Mater., 102 (1981) 192–199.
[10] .J.F. Marinand P. Contamin, J. Nucl. Mater., 30 (1969) 16–25.
[11] H. Matzke, Radiat. Eff. 75 (1983) 317–325.
[12] J. Belle, J. Nucl. Mater., 30 (1969) 3–15.
[13] P. Contamin and R. Stefani, CEA-R-3179 (April 1967).
[14] G.E. Murch and C.R.A. Catlow, J. Chem. Soc. Faraday Trans., 2 (83) (1987) 1157–1169.
[15] B. Dorado, J. Durinck, P. Garcia, M. Freyss and M. Bertolus, J. Nucl. Mater., 400 (2010) 103–106.
[16] E. Yakub, C. Ronchi and D. Staicu, J. Chem. Phys., 127 (2007) 094508.
[17] R. Devanathan, J. Yu and W.J. Weber, J. Chem. Phys., 130 (2009) 174502.
[18] K. Refson, Comput. Phys. Commun., 126 (2000) 310–329.
[19] S. Hull, Rep. Prog. Phys., 67 (2004) 1233–1314.
[20] H. Matzke, Radiat. Eff., 64 (1982) 3–33.
[21] N. Nakae, A. Harada, T. Kirihara and S. Nasu, J. Nucl. Mater., 71 (1978) 314–319.
[22] W.J. Weber, J. Nucl. Mater., 98 (1981) 206–215.
[23] G.E. Murch, Chapter 3 in Diffusion in Crystalline Solids edited by A.S. Nowick, Academic Press, New York, (1984), pp. 143–188.
[24] N.F. Mott and M.J. Littleton, Trans. Faraday Soc., 34 (1938) 485–499.
[25] J.D. Gale and A.L. Rohl, Mol. Simulat., 29 (2003) 291–341.
[26] H. Matzke, J. Less Common. Met., 121 (1986) 537–564.
[27] M.T. Hutchings, J. Chem. Soc., Faraday Trans., 2 (83) (1987) 1083–1103.
[28] W. Breitung, J. Nucl. Mater., 74 (1978) 10–18.
[29] G.E. Murch and R.J. Thorn, J. Nucl. Mater., 71 (1978) 219–226.

Brought to you by | Yildiz Technical University
Authenticated
Download Date | 12/13/18 8:15 AM